Dissecting Ent3p: The ENTH domain binds different SNAREs via distinct amino acid residues while the C-terminus is sufficient for retrograde transport from endosomes

Jana Zimmermann, Subbulakshmi Chidambaram, Gabriele Fischer von Mollard

Revised Version of BJ2010/693

Dissecting Ent3p: The ENTH domain binds different SNAREs via distinct amino acid residues while the C-terminus is sufficient for retrograde transport from endosomes

Jana Zimmermann, Subbulakshmi Chidambaram* and Gabriele Fischer von Mollard
From: Biochemie III, Fakultät für Chemie, Universitätstrasse 25, Universität Bielefeld, 33615 Bielefeld, Germany.
*Current address: Department of Biochemistry and Cell Biology, Sankara Nethralaya Vision Research Foundation, Chennai, India

Address correspondence to: Gabriele Fischer von Mollard, Biochemie III, Fakultät für Chemie, Universitätstrasse 25, Universität Bielefeld, 33615 Bielefeld, Germany.
Tel (49) 521 1062081; Fax: (49) 521 1066014;
E-mail: gabriele.mollard@uni-bielefeld.de

Short title: Ent3p binding to the endosomal SNAREs Vti1p, Pep12p and Syn8p

Key words: membrane traffic, TGN, endosome, Vti1p, Pep12p, Syn8p

Synopsis

The epsin N-terminal homology (ENTH) domain protein Ent3p and the AP-180 N-terminal homology (ANTH) domain protein Ent5p serve as partially redundant adaptors in vesicle budding from the TGN in *Saccharomyces cerevisiae*. They interact with phosphoinositides, clathrin, adaptor proteins and cargo such as chitin synthase Chs3p and SNAREs. Here we show that *ent3Δent5Δ* cells displayed defects in cell separation and bud-site selection. Ent3p and Ent5p were also involved in retrograde transport from early endosomes to the TGN because GFP-Snc1p shifted from a plasma membrane to an intracellular localization in *ent3Δent5Δ* cells. The C-terminal part of Ent3p was sufficient to restore retrograde transport from early endosomes to the TGN in *ent3Δent5Δ* cells. By contrast, ENTH-domain and the C-terminus were required for transport from the TGN to late endosomes demonstrating that both functions are distinct. The ENTH domain of Ent3p is known to bind the N-terminal domains of the SNAREs Vti1p, Pep12p and Syn8p, which are required for fusion with late endosomes. The interaction surface between the Ent3p-related mammalian epsinR and vti1b is known. Here we show that Vti1p bound to the homologous surface patch of Ent3p. Pep12p and Syn8p interacted with the same surface area of Ent3p. However, different amino acid residues in Ent3p were crucial for the interaction with these SNAREs in two-hybrid assays. This provides necessary flexibility to bind three SNAREs with little sequence homology but maintains specificity of the interaction.

Introduction

In eukaryotic cells, vesicles containing cargo bud from donor organelles, are transported to target organelles and fuse with target membranes. Organelles are connected by forward, anterograde transport and reverse, retrograde transport routes. The trans-Golgi network (TGN) is a branching point for protein traffic to the plasma membrane, early endosomes, late endosomes or the vacuole in yeast [1]. Transport routes connect early endosomes with the plasma membrane, the TGN and via late endosomes with vacuoles.

The coat of vesicles trafficking between TGN and endosomes contain structural components like clathrin as well as clathrin binding and cargo sorting components such as adaptor proteins (APs) and Ggas [2]. In addition there are cargo specific adaptors like sorting nexins, ENTH or ANTH domain proteins [3]. The family of epsin N-terminal homology (ENTH) domain proteins has 4 members each in mammals (epsin1-3 and epsinR) and yeast (Ent1-4p). All family members contain the ENTH domain, which folds into a conserved structure with eight α-helices [4, 5] and binds phosphoinositides (PI). The unstructured C-terminus provides a contact surface for other adaptors like Ggas and APs or clathrin. Ent4p contributes to cargo specific transport from the TGN to the vacuole [6]. Ent3p functions at the TGN where it interacts with Gga2p, AP-1 and clathrin in transport to endosomes [7]. Ent3p shows some functional redundancies with the ANTH (AP-180 N-terminal homology) domain protein Ent5p, which interacts with the chitin synthase 3 Chs3p [8, 9]. The ANTH-domain proteins are a family of adaptor like proteins, which are structurally and functionally related to ENTH-domain proteins and can also bind phosphoinositides, clathrin and APs [3]. *ent3Δ* cells show only small or no defects in trafficking but the *ent3Δent5Δ* double mutant cells display defects in sorting of the vacuolar carboxypeptidase Y (CPY), the vacuolar carboxypeptidase S and Chs3p [7, 8]. The chitin synthases Chs1p and Chs3p are partially stored in an early endosomal subfraction called chitosome [10]. Newly synthesized Chs3p is routed from the TGN directly to the plasma membrane where it is involved in the formation of the initial ring at the base of an emerging bud and the synthesis of chitin dispersed in the cell wall [11]. Chs3p gets

endocytosed and starts cycling between plasma membrane, chitosomes and the TGN [12].

Membrane anchored SNARE proteins play an essential role on both membranes in mediating fusion [13]. Four SNARE motifs from three or four SNARE proteins have to build a complex of four different α-helices. The interior of the SNARE complex consists of 15 hydrophobic layers of interacting amino acid side chains. The central hydrophilic 0-layer contains one arginine (R) and three glutamines (Q). According to this residue and amino acid homologies SNAREs can be classified into four different subfamilies R, Qa, Qb and Qc-SNAREs. One SNARE of each subfamily is found in a functional SNARE complex. To maintain the SNARE concentration on budding vesicles, SNAREs have to be recycled after vesicle fusion. Sorting determinants for SNAREs can consist of the transmembrane domain, linear amino acid sequences or conformational motifs in the N-terminus [14-16]. The mammalian Ent3p ortholog epsinR interacts with the Q-SNARES vti1b, syntaxin 7, and syntaxin 8 [17], which function together in fusion with the late endosome and lysosome [18, 19]. The ENTH domain of epsinR interacts with the N-terminus of vti1b via a conformational motif, which includes at least 2 turns and one helix of epsinR and amino acid residues from three helices of vti1b [5]. Binding to epsinR is required for sorting of vti1b into clathrin coated vesicles [20]. These interactions are conserved between yeast and mammals. Ent3p binds the Q-SNAREs Vti1p, Pep12p and Syn8p [17, 21], which participate in fusion with the late endosome [22-24]. Close homologies are shared between Vti1p and vti1b, Pep12p and syntaxin 7 as well as Syn8p and syntaxin 8. The localization of Vti1p and Pep12p is dependent on Ent3p together with the partially redundant Ent5p indicating that the cargo sorting function of Ent3p is conserved in yeast and extends to more than one SNARE [8, 17].

Here we set out to characterize the interaction surface of Ent3p with these three yeast SNAREs. We wanted to find out whether Syn8p is also a cargo. As mammalian epsinR is required for retrograde transport from the early endosome to the TGN we studied this transport step in *ent3Δent5Δ* cells. Effects on the cell separation and on budding patterns were investigated because proteins involved in these processes cycle through early endosomes and TGN. In addition, we wanted to determine the role of Ent3p domains in different functions.

Experimental

Materials

Reagents were obtained from the following sources: enzymes for DNA manipulation from New England Biolabs (Beverly, MA), zymolyase from Seikagaku (Tokyo, Japan) and FM4-64 from Invitrogen (Carlsbad, CA, U.S.A.). All other reagents were purchased from Sigma (St Louis, MO). Plasmid manipulations were performed in *E. coli* strains XL1blue or DH5α using standard media. Yeast strains (Table 1) were grown in rich medium (1% yeast extract, 1% peptone, 2% dextrose, YEPD) or standard minimal medium (SD) with appropriate supplements.

Strains and plasmids

Single deletion strains in BY4742 background were obtained from the Euroscarf strain collection [25]. Diploid BY wild-type (WT) cells were obtained by mating of BY4742xBY4741 and selection on -Met -Lys SD plates. Diploid *ent3*Δ*ent5*Δ cells were constructed by mating BKY13 with SCY34 in which the BKY13 mating type was switched via the transformation of the pGAL-HO plasmid [26].
Plasmids used in this study are described in table 2. ENTH/ANTH chimeras were constructed

via PCR with bridging primers and Ent3p point mutants with two PCRs using overlapping mutant oligos containing the mutation and sequences complementary to the *ENT3* gene in the first PCR. In the second PCR the overlapping products of the first PCR were amplified to one construct and cloned into the target vectors with standard cloning techniques. 3xHA tagged Ent3p C-terminus and Syn8p were constructed by insertion of a BglII restriction site after the ATG and subcloning of the 3xHA fragment from pSM492 [27] into the vector via BglII.

Budding analysis

Bud scars are chitin-rich regions where the daughter cell was separated from the mother cell and which can be visualized by calcofluor white staining [28]. For the staining 20 ml yeast cells in mid-logarithmic phase were fixed by adding formaldehyde to a final concentration of 3.7% and incubated for 30 min at 30°C. The fixed cells were pelleted, resuspended in 4% formaldehyde in PBS and incubated again for 30 min at room temperature. The cells were washed with PBS and resuspended in 500 µl PBS. 15 µl 1 mg/ml Calcofluor white (in H_2O) were added to 100 µl cell suspension. The incubation was carried out for 5 min in the dark. The cells were washed three times with PBS, resuspended in 10 µl mounting medium and bud scars were visualized by fluorescence microscopy. Each cell was photographed in three focal planes to ensure that all bud scars and cell-cell-connections were imaged. For quantification of the budding pattern cells with two or more buds were counted as wild-type if the bud scars were not more than one bud scar length apart in haploids and clearly assignable to the cell poles in diploids.

CPY secretion assay

Secretion of CPY resulting from a defect in TGN to vacuole transport was analyzed as described [29]. Yeast cells were grown into logarithmic stage, spotted onto a YEPD agar plate, incubated 24 h at 30°C and further incubated for 24h covered with a nitrocellulose membrane at 30°C. The washed nitrocellulose membrane was treated with mouse-anti-CPY antibody (kindly provided by T. Stevens, University of Oregon, USA), HRP-conjugated anti-mouse antibody (Dianova) and ECL substrate (Thermo Fisher Scientific, Rockford, U.S.A.).

Fluorescence microscopy

Yeast cells were grown to an early logarithmic stage (GFP-Snc1p localization [15]) or logarithmic stage (GFP-Yck2p [30]) in appropriate SD minimal medium at 30°C. For FM4-64 staining of vacuoles, approx. 0.7 absorbance units of cells were pelleted and resuspended in 120 µl of YEPD, and 1 µl of 16 mM FM4-64 was added. After 30 min incubation at 30°C, cells were washed once with YEPD and immediately viewed under a fluorescence microscope (Leica DM-5000 B) with the Leica DFC350 FX CCD camera (charge-coupled-device camera). For GFP–Snc1p and GFP-Yck2p localization, cells were pelleted, resuspended in PBS and immediately viewed under a fluorescence microscope.

Yeast two-hybrid assays

The yeast two-hybrid assay was performed as described [31] in L40 cells using pLexN with the N-terminal domain of SNARES as bait vectors, and the ENTH domain of Ent3p or mutated ENTH constructs in pVP16-3 as prey vector. Yeast cells containing pairs of LexA DNA binding domain and VP16 activation domain fusions were streaked out on agar plates lacking tryptophan, uracil, leucine, lysine and histidine (THULL, Vti1p with chimera), which were supplemented with 1 mM 3-aminotriazole (other SNAREs with chimera) or 2 mM 3-aminotriazole (SNAREs and point mutants) to detect expression of the reporter HIS3 and in parallel on plates lacking tryptophan and leucine to confirm viability. The VP16 activation domain served as negative control (pVP) for unspecific activation by LexA-SNAREs. ENTH

and ANTH constructs did not cause nonspecific activation as tested in combination with a LexA-laminin fusion protein. Expression of the constructs was confirmed by Western blotting.

Subcellular fractionation

Subcellular fractionation was performed by sucrose density gradient centrifugation. Wild-type, *ent3*Δ*ent5*Δ (BKY13) and *ent3*Δ*ent5*Δ cells containing Ent3p point mutation plasmids (pJZ17, pJZ18, pCP13) expressing HA-Syn8p from a CEN plasmid under endogenous promoter (pJZ21) were spheroplasted, osmotically lysed and centrifuged at 500 *g* to remove debris. The homogenates were separated by sucrose density centrifugation [22]. The gradient consisted of the following steps: 0.5 ml 55%, 1.0 ml 42%, 1.0 ml 37%, 1.5 ml 34%, 2.0 ml 32%, 1.5 ml 29%, 1.0 ml 27%, 1.0 ml 22% (w/w) sucrose in 10 mM HEPES-NaOH pH 7.6, with centrifugation for 16 hours at 135,000 g_{max} (27,000 r.p.m in an AH627 rotor). Fractions were separated by SDS-PAGE and immunoblotted using antisera against Vti1p, Pep12p, Use1p [17, 24, 32], monoclonal antibodies against HA (HA.11 clone 16B12, Covance), 100 kDa subunit of the vacuolar ATPase, phosphoglycerate kinase (both Invitrogen), Pma1p (clone 40B7, Lifespan Biosciences), HRP-conjugated secondary antibodies (Dianova) and ECL substrate (Pierce).

Membrane association

For analysis of the Ent3p membrane association a subcellular fractionation via differential centrifugation was performed as described previously [33]. Yeast cells were washed with cold lysis buffer (20 mM HEPES pH 6.8, 150 mM potassium acetate, 10 mM magnesium chloride and 250 mM sorbitol), resuspended in ice cold lysis buffer supplemented with protease inhibitors and lysed by vortexing in glass tubes containing glass beads. The lysates were centrifuged at 500 *g* and the supernatant (homogenate, H) was further centrifuged at 13,000 *g*. The resulting pellet (P13) was resuspended in lysis buffer with protease inhibitors and the supernatant centrifuged at 200,000 *g* (pellet = P200, supernatant = S200). The H, P13, P200 and S200 fractions were separated by SDS-PAGE and immunoblotted using antisera against Ent3p, Vti1p, Use1p [17, 24, 32], monoclonal antibodies against HA (HA.11 clone 16B12, Covance), phosphoglycerate kinase (Invitrogen) HRP-conjugated antibodies, ECL substrate and a CCD camera (Fujifilm LAS 3000). For calculation of membrane bound Ent3p the band intensities were quantified and the sum of intensities in P13 and P200 was divided by the sum of intensities P13, P200 and S200.

Results

Absence of Ent3p and Ent5p resulted in defective budding pattern and cell separation.

We tested whether the lack of Ent3p and Ent5p had such an impact on trafficking of proteins involved in bud site selection and cell separation that defects in these processes could be observed in *ent3*Δ*ent5*Δ cells. After separation of the daughter cell from the mother cell a ring like chitin accumulation (so called bud scar) remains on the mother cell. These bud scars can be visualized with Calcofluor white staining [28]. Diploid and haploid *ent3*Δ*ent5*Δ and wild-type (WT) cells were stained with Calcofluor white. Cells with two or more bud scars were examined for budding pattern by fluorescence microscopy. The selection of the bud site follows a specific pattern [34, 35]. The new bud emerges next to the last bud scar (axial budding pattern) in haploid cells. In diploid cells however the new bud forms on the opposite cell pole (bipolar budding pattern). In the diploid *ent3*Δ*ent5*Δ yeast strain 52% of the cells showed an abnormal budding pattern (Fig. 1A and 1B). In diploid WT cells only 17%

deviated from the typical bipolar budding pattern. A defect was observed but less pronounced in haploid cells. 36% of the double mutant cells did not display the expected axial budding pattern in comparison to 4% of the wild-type cells. *ent3*Δ and *ent5*Δ single mutant haploid cells had no defects in bud site selection (data not shown). Haploid and diploid cells were analyzed for cell separation defects. The same diploid *ent3*Δ*ent5*Δ cells photographed in three different focal plains are shown in Fig. 1C. White arrows indicate two connected cells each with a new bud. 21% of the haploid *ent3*Δ*ent5*Δ cells had more than one bud (Fig. 1D and 1E). 2% multibudded cells were counted for the WT strain.

_ent3_Δ_ent5_Δ cells were defective in retrograde transport from early endosomes to the TGN.

Mammalian epsinR is involved in retrograde transport from early endosomes to the TGN [36]. An involvement of Ent3p and Ent5p in this retrograde transport step has not been tested yet. We used a cargo for the early endosome to TGN assay, which is not transported from the TGN to endosomes because transport from the TGN to endosomes is delayed or partially blocked in *ent3*Δ*ent5*Δ cells. The R-SNARE Snc1p is required on TGN derived secretory vesicles for fusion with the plasma membrane. Snc1p is localized predominately to the plasma membrane (PM) and is recycled via early endosomes back to the TGN. The GFP-Snc1p construct is a useful and established tool for analyzing this retrograde transport to the TGN. A block in this recycling step causes an intracellular accumulation of GFP-Snc1p in endosomal structures [15].

In *ent3*Δ*ent5*Δ cells the GFP-Snc1p was almost completely mislocalized and only 4% of the cells had an accumulation on the plasma membrane (Fig. 2A and D). By contrast 83% of the WT cells showed a plasma membrane staining. A high amount of the GFP-Snc1p was localized to the vacuole membrane visualized by FM4-64 staining in the double mutant cells (Fig. 2C). In addition the *ent3*Δ or *ent5*Δ single mutant cells had slight defects in GFP-Snc1p recycling (*ent3*Δ: 64%, *ent5*Δ: 68% of the cells had plasma membrane staining).

The yeast casein kinase 1 isoform Yck2p is another protein, which functions at the plasma membrane and which localization is dependent on cycling through endosomes. The yeast casein kinases Yck1p and Yck2p play roles in cell morphogenesis, cytokinesis, bud-site selection and endocytosis [37-39]. The localization of Yck2p at the plasma membrane is dependent on the SNARE Tlg2p [40], which functions in fusion with the TGN in a SNARE complex containing also Snc1/2p, Tlg1p and Vti1p. Here we show that the localization of Yck2p depends also on the adaptor proteins Ent3p or Ent5p. In *ent3*Δ*ent5*Δ cells the GFP-Yck2p is partially mislocalized to the vacuolar membrane (Fig. 2B and E). Clear vacuolar staining can be observed in 25% of the *ent3*Δ*ent5*Δ cells, but only in 2% of the wild type cells. The fragmented vacuole phenotype of the *ent3*Δ*ent5*Δ double mutant underlines this defect. The *ent3*Δ or *ent5*Δ single mutant cells showed a wild-type distribution of Yck2p. These data indicate that *ent3*Δ*ent5*Δ cells were defective in retrograde transport from early endosomes to the TGN.

Characterization of the interaction surface between Ent3p and the endosomal SNAREs.

One important function of Ent3p is cargo sorting of the endosomal SNAREs Vti1p, Pep12p and Syn8p. We were interested to analyze the amino acid residues of Ent3p important for the binding of three different SNAREs. As the first tool chimeric proteins were generated with sequences of the ANTH protein Ent5p, which does not bind Vti1p, Pep12p or Syn8p [17]. Full length Ent5p did not interact with these SNAREs in two hybrid assays either (Suppl. Fig. 1). The contribution of the Ent3p N-terminal region encompassing predicted helices α0 – α5 and C-terminal regions with helices α6 - α8 was analyzed by combining them with Ent5p

sequences contributing the missing helices (Fig. 3A, B). Exchanging Ent3p AA113-172 with Ent5p AA112-172 (ChimA) or Ent3p AA1-112 with Ent5p AA1-111 (ChimB) abolished interactions between Ent3p and Vti1p, Pep12p or Syn8p in a yeast-two-hybrid assay (Fig. 3C). Chimeras with Ent3p helices α0 – α6 (Ent3p AA1-126 Ent5p AA130-172) or Ent3p helices α4 – α8 (Ent5p AA1-82 Ent3p AA83-172) did not interact with the SNAREs either (data not shown). Our data indicate that Vti1p, Pep12p and Syn8p interactions or correct folding require amino acids in different areas of the ENTH domain. In the mammalian system the Ent3p orthologue epsinR interacts with vti1b, syntaxin 7 and syntaxin 8. In earlier studies we showed that Vti1p does not interact with epsinR and vti1b not with Ent3p, respectively [21]. To determine which parts of the Ent3p and epsinR ENTH domain are responsible for species specific interactions, appropriate constructs were generated and tested by yeast-two-hybrid assays. In the yeast-two-hybrid assay with the chimeric constructs we still found interactions of vti1b with epsinR AA1-104 Ent3p AA113-172 (Chim D) and a very weak interaction of Vti1p with Ent3p AA1-113 epsinR AA105-162 (Chim C, Fig. 3B, C). By contrast, Chim C with epsinR helices α6 - α8 did not interact with vti1b and Chim D with Ent3p helices α6 - α8 did not bind Vti1p. An extremely weak growth was detected for cells containing Pep12p or Syn8p constructs with chimera C but not other chimera in a few experiments. Therefore helices α0 – α5 seem to contribute more to the species specific interaction. The last 3 helices of the ENTH domain can be exchanged between mammals and yeast without weakening of the interaction for vti1b and with retention of low binding capacity for Vti1p. However, epsinR helices α6 - α8 should also contribute to the interaction with Vti1p as Chim A with Ent5p helices α6 - α8 does not interact. In addition, Pep12p and Syn8p have similar but not identical requirements to Vti1p.

The interaction between epsinR and vti1b was characterized by solving the crystal structure of the epsinR-vti1b complex and experiments with amino acid exchanges [5]. The interaction surface of epsinR with vti1b is a conformational motif, which needs especially the regions between helices α2 and α3, α4 and α5 and several amino acids on helix α8. The structure of Ent3p was modeled with 3D-Jigsaw using the epsinR crystal structure (Fig. 3D) and modeled into the complex with vti1b (Fig. 3E, red) to investigate whether equivalent amino acid residues are required for Vti1p binding and whether the same amino acid residues are also crucial for interactions with Pep12p and Syn8p. The amino acids exchanges Y60D, F62D, E103W and R154E in Ent3p were chosen from sequence and structure alignment to the mammalian epsinR/vti1b complex and epsinR mutational analysis. In epsinR homologous mutations F52D (Y60 in yeast Ent3p), M53D/Y54D (Y54 equivalent to F62 in Ent3p) and R146E (R154) inhibited the interaction with vti1b [5]. We also exchanged the amino acid E103 to tryptophan, which did not abolish the epsinR interaction to vti1b in the mammalian system (E95W). We could demonstrate that in the yeast complex equivalent amino acids were necessary for the interaction of Vti1p with Ent3p (Fig. 3F). No interactions of the Vti1p N-terminus with the Ent3p Y60D, F62D and R154E mutants were detectable in the yeast two-hybrid system. EpsinR E95W and Ent3p E103W still interacted. Pep12p and Syn8p displayed a different interaction pattern from each other and from Vti1p. The interaction with Pep12p was abrogated in all four Ent3p mutants. Syn8p did not interact with the Ent3p mutants E103W and R154E. The results implicate that the Pep12p and Syn8p bind to the same interaction surface of Ent3p as Vti1p but each of these SNAREs requires a set of different amino acid residues. Of four amino acid residues tested only R154 was important for binding of all three SNAREs.

In vivo effects of Ent3p point mutants.

In *ent3*Δ*ent5*Δ cells Vti1p and Pep12p are shifted to denser fractions of a sucrose density

gradient compared to wild-type cells [8, 17]. The third Q-SNARE of the complex HA-Syn8p was also mislocalized to denser fractions in the double mutant cells (Fig. 4A). We analyzed the distribution of these SNARE proteins in vivo using Ent3p point mutants, which prevent two-hybrid interactions with two (Y60D, E103W) or three (R154E) SNAREs. The Ent3p point mutants Y60D, E104W and R154E were expressed under the endogenous promoter in *ent3*Δ*ent5*Δ cells. Expression levels of mutant and wild-type Ent3p were similar (Suppl. Fig. 2). HA-Syn8p, Pep12p and Vti1p protein levels were comparable in wild-type, *ent3*Δ*ent5*Δ and *ent3*Δ*ent5*Δ cells expressing these Ent3p point mutants by Western blotting (Suppl. Fig. 2) suggesting the absence of massive vacuolar degradation due to mislocalization. Expression of *ent3-E103W* with a mutation not affecting interaction with Vti1p (Fig. 3F) in *ent3*Δ*ent5*Δ cells returned Vti1p to the position in the gradient observed in *ent5*Δ and wild-type cells (Fig. 4B, C). Ent3 Y60D could not bind Vti1p in the two-hybrid assay but surprisingly *ent3-Y60D* still corrected the localization of Vti1p in the sucrose gradient in *ent3*Δ*ent5*Δ cells. In addition, Pep12p was not significantly mislocalized in *ent3-Y60D* or *ent3-E103W* expressing *ent3*Δ*ent5*Δ cells even though Y60D and E103W disrupted the two-hybrid interaction (Fig. 4D). Only when the interaction with all three SNAREs was blocked by the R154E amino acid exchange in the two-hybrid system Pep12p remained in the denser fractions as observed for *ent3*Δ*ent5*Δ cells (Fig. D). The distribution of markers for ER, plasma membrane and vacuoles was similar after fractionation of wild-type, *ent3*Δ*ent5*Δ and *ent3*Δ*ent5*Δ cells expressing *ent3-R154E* (Suppl. Fig. 2). HA-Syn8p was shifted to lighter fractions even in the presence of *ent3-R154E* (Fig. 4A). For Vti1p the defect upon expression of *ent3-R154E* was less pronounced compared to *ent3*Δ*ent5*Δ cells (Fig. 4B). In summary, SNARE sorting was less affected by the point mutations than expected by the two-hybrid assays but some defects were observed.

To determine whether the *ent3p* point mutants were able to complement the early endosome to TGN trafficking defects these proteins were expressed in *ent3*Δ*ent5*Δ cells and analyzed for GFP-Snc1p localization. All four *ent3p* point mutants were able to restore the defect in GFP-Snc1p localization almost to the level observed in *ent5*Δ cells (Fig. 4E). These data indicate that these point mutations are functional in retrograde traffic to the TGN. Ent3p has a role in trafficking of the vacuolar soluble hydrolase carboxypeptidase Y (CPY) [7, 8, 21]. CPY is bound by its sorting receptor Vps10p in the TGN. After transport to the late endosome Vps10p is recycled to the TGN for the next round of cargo sorting and CPY is further transported to the vacuole [1]. Due to a partial block in transport CPY is secreted slightly in *ent3*Δ and stronger *ent3*Δ*ent5*Δ cells. Secretion of CPY was detected in an overlay assay. *ent3*Δ cells overexpressing *ENT3* and *ent5*Δ cells transported CPY correctly to the vacuole and almost no secretion of CPY occurred (Fig. 4F). Expression of *ent3-R154E, ent3-F62D* or *ent3-E103W* could not rescue the CPY secretion defect of *ent3*Δ*ent5*Δ cells (Fig. 4F). The *ent3-Y60D* mutant was difficult to analyze since it had a strong growth defect at all temperatures (data not shown). Although most Vti1p, Pep12p and Syn8p was localized correctly in *ent3*Δ*ent5*Δ cells expressing *ent3-E103W* the sorting may be not efficient enough for perfect transport.

Absence of different Ent3p domains caused distinct phenotypes.

As the *ent3p* point mutants were functional in retrograde transport to the TGN we set out to determine which parts of Ent3p are required for this transport step and for CPY transport. The Ent3p the C-terminus interacts with clathrin adaptors Gga2p and AP-1. The Ent3p ENTH domain binds SNAREs and phosphatidylinositides (PI). Three basic residues in the α0 helix at the N-terminus of the epsin 1 ENTH domain are essential for PI binding [4, 41]. The N-terminus of Ent3p contains four basic residues, three in the same spacing as in epsin 1

suggesting that it is also required for PI binding. However, SNARE binding does not require the 19 N-terminal amino acid residues of epsinR, the mammalian Ent3p ortholog [5].

We constructed overexpression plasmids coding for either the Ent3p ENTH domain (ENTH), the C-terminus (C-Term) or the full length protein without the N-terminal amino acids 1-28 predicted to form the α0 helix (-PI) and transformed them into *ent3*Δ*ent5*Δ cells. Since the membrane binding capacity of Ent3p may be crucial for function we checked the membrane association via differential centrifugation of yeast cell homogenates (Fig. 5A). As observed before membrane associated Ent3p is found predominantely in the low speed membrane fraction P13 [42]. The percentage of -PI Ent3p in the membrane fractions P13 and P200 was slightly reduced to 32% from 42% in *ent3*Δ cells overexpressing *ENT3* from a *2μ* plasmid. This residual binding must be mediated through interactions with membrane bound proteins such as SNAREs (interact with ENTH) or Gga2p (interacts with C-terminus). Full length Ent3p and Ent3p ENTH (49%) showed comparable membrane binding. 20% of the Ent3p C-terminus was bound to the P13 and P200 membranes, a significant reduction but some membrane association was still possible. Upon overexpression of either the Ent3 C-terminus or the Ent3p ENTH domain alone *ent3*Δ*ent5*Δ cells secreted similar amounts of CPY as in the absence of these Ent3p constructs (Fig. 5B). As Ent3p C-terminus or the Ent3p ENTH domain were not able to rescue the transport defect both domains are required for CPY transport. In addition, neither ENTH domain nor C-terminus were able to correct the subcellular distribution of Vti1p or Pep12p in sucrose density gradients in *ent3*Δ*ent5*Δ cells (data not shown). Overexpression of Ent3p without the potential α0 helix required for PI binding reduced CPY secretion in *ent3*Δ*ent5*Δ cells. However, we observed only a partial complementation with higher CPY secretion than in *ent5*Δ cells indicating that the -PI mutant Ent3p construct had partial function. The reduction of membrane association in the -PI mutant Ent3p may be enough to cause the slight CPY secretion. These data indicate that the ENTH domain was required while PI binding was less important for CPY transport.

Overexpression of just the Ent3p ENTH domain in *ent3*Δ*ent5*Δ cells resulted only in a minor suppression of the GFP-Snc1p mislocalization (14% cells with plasma membrane staining as seen in Fig. 6A and B). Overexpression of the Ent3p C-terminus complemented the defect to a level almost comparable to *ent5*Δ cells (50% PM staining). From these results we can conclude that the Ent3p C-terminus is crucial for the GFP-Snc1p trafficking while the ENTH domain is not required. Presence of the Ent3p-PI plasmid, which contains the whole C-terminus also rescued the defect almost to a single mutant level (51% PM staining).

The GFP-Yck2p distribution in *ent3*Δ*ent5*Δ cells containing only the Ent3p ENTH domain was comparable to the double mutant cells and also showed a fragmented vacuole phenotype (Fig. 6A and C). By contrast, expression of the Ent3p C-terminus or Ent3p -PI complemented the GFP-Yck2p recycling defect of *ent3*Δ*ent5*Δ cells considerably. These data indicate that the Ent3p C-terminus was sufficient and the ENTH domain not essential for retrograde traffic from early endosomes to the TGN.

Discussion

Lack of Ent3p and Ent5p results in delays and slight defects in transport from the TGN to the late endosome [7, 21] and in sorting into multivesicular bodies [42]. In addition, *ent3*Δ*ent5*Δ cells retain the chitin synthase Chs3p in the TGN [8]. Here, we used an established assay to analyze retrograde transport from the plasma membrane via early endosomes to the TGN [15]. We found an almost complete shift of GFP-Snc1p from the plasma membrane to an intracellular localization in *ent3*Δ*ent5*Δ cells demonstrating a strong defect in retrograde transport to the TGN. *ent3*Δ or *ent5*Δ single mutant cells had a slight loss of GFP-Snc1p

plasma membrane staining indicating that Ent3p and Ent5p are partially redundant in retrograde transport to the TGN. Ent5p related sequences have so far been identified only in species closely related to *Saccharomyces*. This means that the function of Ent3p and epsinR, the closest mammalian homolog of Ent3p, is more conserved in evolution than previously demonstrated. EpsinR is involved in retrograde transport from early endosomes to the TGN [36] while transport from the TGN to late endosomes has not been tested.

The casein kinase Yck2p was also mislocalized from the plasma membrane to internal stores in *ent3*Δ*ent5*Δ cells confirming the block in retrograde transport from endosomes to the TGN. In vitro, Yck2p is able to phosphorylate many substrates including Ent5p, the chitin synthase Chs1p and Chs4p/Skt5p, which activates Chs3p and recruits it to the bud neck [43]. Mislocalization of Chs3p and Yck2p could cause the defects we observed in budding pattern and in increased numbers of multibudded cells in the absence of Ent3p and Ent5p. Chs3p is responsible for deposition of chitin in the cell wall and in a ring, where the bud emerges [44]. Lack of Chs3p and Chs1p results in abnormal deposition of chitin, changes in cell shape and cells with multiple buds [44]. As both Chs3p and Chs1p recycle between the plasma membrane and an endosomal compartment [10], it is likely that Chs1p is also mislocalized in *ent3*Δ*ent5*Δ cells. Temperature sensitive loss of casein kinase I activity, which is provided by Yck1p and Yck2p leads to cells with multiple, elongated buds and several nuclei [38]. At permissive temperature *yck1*Δ*yck2-ts* cells have normal morphology but an increase in abnormal budding pattern in the haploid and diploid state [37]. Mislocalization of Yck2p may cause the bud site selection defect in haploid and diploid *ent3*Δ*ent5*Δ cells. Defects in several genes linked to the actin cytoskeleton and to transport in the endosomal system result in changes in bud site selection in diploid cells as these factors are required for correct targeting of bipolar cortical landmarks [34, 35, 45]. Therefore the stronger defect in bud site selection in *ent3*Δ*ent5*Δ diploid cells may follow the same mechanism as in *vps45*Δ or *vps54*Δ (also called *luv1*) cells, because both proteins are involved in retrograde traffic from endosomes to the TGN.

For epsins involved in endocytosis expression of the ENTH domain alone is necessary and sufficient to correct defects in yeast [46] and in *Dictyostelium* [47]. In Drosophila, the expression of either ENTH domain or C-terminus of the endocytic ENTH protein Liquid facets is sufficient for complementation [48]. We found that expression of the Ent3p ENTH domain was not sufficient to rescue retrograde transport from early endosomes to the TGN. Surprisingly, this defect was complemented by expression of the Ent3p C-terminal domain. The ENTH domain was reported to be required for Ent3p membrane binding [42]. In our strain background, substantial membrane binding remained in the absence of the ENTH domain. AP-1 and Gga1/2p most likely serve as membrane anchors for Ent3p in the absence of the ENTH domain because they bind to the Ent3p C-terminal domain and associate with membranes in budding of clathrin coated vesicles. A functional complementation by the C-terminus indicates that Ent3p may stabilize a local network of proteins via AP-1 and Gga1/2p to improve the budding process. By contrast, the TGN to late endosome transport defect in CPY sorting was not complemented by an Ent3p construct lacking the ENTH domain but partially rescued by a construct lacking the N-terminal amino acid residues 2-27. In epsin 1 these residues are essential for phosphoinositide binding [41] but corresponding residues in epsinR are not required for interaction with vti1b [5]. Ent3p point mutations showed that the Ent3p C-terminus is not sufficient for correct sorting of Vti1p and Pep12p. These data indicate that SNARE interactions are required for an optimal function of Ent3p in CPY traffic.

The interaction face between the mammalian epsinR ENTH domain and the vti1b N-terminus has been characterized by protein crystallography and point mutations [5]. In epsinR about 15 amino acid residues from different parts of the molecule contribute to the interaction surface.

Most important are the loops between helix α2 and α3 and between helix α4 and α5 as well as helix α8. The N-terminus of vti1b consists of a bundle of three α-helices. About 15 amino acid residues from all helices contribute to the interaction surface. The N-terminus of Vti1p is highly α-helical ([49], our unpublished observations) and should also form a three helix bundle even though Vti1p shares only 16% identical and 42% similar amino acid residue in this domain. While most amino acid residues in the interaction surface of epsinR are identical or conserved in Ent3p, many interacting amino acid residues in vti1b are not conserved in Vti1p [5]. Our data indicate that the interaction surface in Ent3p is similar to that in epsinR. Experiments with chimeric molecules between the ENTH domain of Ent3p and the ANTH domain of Ent5p indicate that large portions of Ent3p are required for interaction. Point mutations in four tested conserved residues in Ent3p had the same effect on Vti1p interaction as in the mammalian system. However, the interaction surface is species specific as there is no interaction between Ent3p and vti1b or epsinR and Vti1p [21]. The most important amino acid residues contributing to species specific binding are localized in helices α0 – α5 as indicated by chimeras between Ent3p and epsinR. Structural information is lacking for the interaction of an ENTH domain with a Qa SNARE such as Pep12p or a Qc SNARE such as Syn8p. The N-terminal domain of Pep12p is almost certainly a three helix bundle because this is observed for all other characterized Qa SNAREs including Vam3p as closest homolog [50]. The N-terminal domain of the Qc SNARE Syn8p should also form a three helix bundle as it is related to Tlg1p and syntaxin 6, which adopt this structure [51, 52]. Therefore the N-termini of Vti1p, Pep12p and Syn8p should have a similar overall structure even though the amino acid sequences are very different. By testing four Ent3p point mutations we found that Vti1p, Syn8p and Pep12p bound to a similar surface patch on Ent3p. However, different amino acid residues in Ent3p contribute to different degrees to binding of these three SNAREs. In this way, the interaction is flexible enough to accommodate interactions with different amino acid residues in these SNAREs.

In *ent3Δent5Δ* cells sorting of Pep12p and Vti1p was not corrected upon expression of *ent3-R154E*, an amino acid exchange, which abolished two-hybrid interaction to Vti1p, Pep12p and Syn8p. These data demonstrate the functional significance of binding to the Ent3p ENTH domain for Vti1p and Pep12p localization. Sorting of Syn8p was less affected in *ent3-R154E ent3Δent5Δ* cells than in *ent3Δent5Δ* cells indicating that the *ent3-R154E* mutant protein had some residual sorting activity for Syn8p even though a two-hybrid interaction was not detected. The sorting defects of Vti1p and Pep12p were corrected by expression of *ent3-Y60D*, which interacted only with Syn8p in the two-hybrid assay. A possible mechanism would be that Vti1p, Pep12p and Syn8p are sorted as a complex by interaction of Syn8p with Ent3p. However, expression of *ent3-Y60D* in *ent3Δent5Δsyn8Δ* cells still corrected the sorting of Pep12p and Vti1p (data not shown). Residual binding to *ent3-Y60D* or additional proteins connecting Vti1p, Pep12p and Ent3p could also be responsible. In mammalian cells, vti1b and Syn8p related syntaxin 8 may be sorted together because syntaxin 8 is missorted to lysosomes in the absence of vti1b [53]. There is already one example for sorting of a SNARE complex into budding vesicles. The COPII coat recognizes a Sed5p/Bos1p/Sec22p SNARE complex at the ER [14]. However, there are three binding sites for SNAREs in the Sec23/24 subcomplex of COPII and different short linear motifs of SNAREs are recognized. By contrast, a large conformational interaction surface mediates the interaction between an ENTH domain and SNAREs allowing for both specificity and binding of three different SNAREs.

Acknowledgments

We thank Claudia Prange and Christiane Wiegand for excellent technical assistance. Lasse Schindler and Andrea Nolting are acknowledged for the construction of plasmids. We thank

TH Stevens (University of Oregon, Eugene, OR, USA) HRB Pelham (MRC Cambridge, UK) and LC Robinson (Louisiana State University, Shreveport, LA, USA) for the gift of antibodies and plasmids. This work was supported by grant GRK 521 from the DFG to GFvM.

References

1 Bowers, K. and Stevens, T. H. (2005) Protein transport from the late Golgi to the vacuole in the yeast Saccharomyces cerevisiae. Biochim. Biophys. Acta **1744**, 438-454
2 Owen, D. J., Collins, B. M. and Evans, P. R. (2004) Adaptors for clathrin coats: Structure and function. Ann. Rev. Cell Dev. Biol. **20**, 153-191
3 Legendre-Guillemin, V., Wasiak, S., Hussain, N. K., Angers, A. and McPherson, P. S. (2004) ENTH/ANTH proteins and clathrin-mediated membrane budding. J. Cell Sci. **117**, 9-18
4 Ford, M. G. J., Mills, I. G., Peter, B. J., Vallis, Y., Praefcke, G. J. K., Evans, P. R. and McMahon, H. T. (2002) Curvature of clathrin-coated pits driven by epsin. Nature. **419**, 361-366
5 Miller, S. E., Collins, B. M., McCoy, A. J., Robinson, M. S. and Owen, D. J. (2007) A SNARE-adaptor interaction is a new mode of cargo recognition in clathrin-coated vesicles. Nature. **450**, 570-U521
6 Deng, Y., Guo, Y., Watson, H., Au, W. C., Shakoury-Elizeh, M., Basrai, M. A., Bonifacino, J. S. and Philpott, C. C. (2009) Gga2 Mediates Sequential Ubiquitin-independent and Ubiquitin-dependent Steps in the Trafficking of ARN1 from the trans-Golgi Network to the Vacuole. J. Biol. Chem. **284**, 23830-23841
7 Duncan, M., Costaguta, G. and Payne, G. (2003) Yeast epsin-related proteins required for Golgi-endosome traffic define a gamma-adaptin ear-binding motif. Nat. Cell Biol. **5**, 77-81
8 Copic, A., Starr, T. and Schekman, R. (2007) Ent3p and Ent5p Exhibit Cargo-specific Functions in Trafficking Proteins between the Trans-Golgi Network and the Endosomes in Yeast. Mol. Biol. Cell. **18**, 1803-1815
9 Costaguta, G., Duncan, M. C., Fernandez, G. E., Huang, G. H. and Payne, G. S. (2006) Distinct roles for TGN/endosome epsin-like adaptors Ent3p and Ent5p. Mol. Biol. Cell. **17**, 3907-3920
10 Ziman, M., Chuang, J. S. and Schekman, R. W. (1996) Chs1p and Chs3p, two proteins involved in chitin synthesis, populate a compartment of the Saccharomyces cerevisiae endocytic pathway. Mol. Biol. Cell. **7**, 1909-1919
11 Chuang, J. S. and Schekman, R. W. (1996) Differential trafficking and timed localization of two chitin synthase proteins, Chs2p and Chs3p. J. Cell Biol. **135**, 597-610
12 Valdivia, R. H., Baggott, D., Chuang, J. S. and Schekman, R. W. (2002) The yeast clathrin adaptor protein complex 1 is required for the efficient retention of a subset of late Golgi membrane proteins. Dev. Cell. **2**, 283-294
13 Jahn, R. and Scheller, R. H. (2006) SNAREs - engines for membrane fusion. Nat. Rev. Mol. Cell Biol. **7**, 631-643
14 Mossessova, E., Bickford, L. C. and Goldberg, J. (2003) SNARE selectivity of the COPII coat. Cell. **114**, 483-495
15 Lewis, M. J., Nichols, B. J., Prescianotto-Baschong, C., Riezman, H. and Pelham, H. R. B. (2000) Specific retrieval of the exocytic SNARE Snc1p from early yeast endosomes. Mol. Biol. Cell. **11**, 23-38
16 Black, M. and Pelham, H. (2000) A selective transport route from Golgi to late

endosomes that requires the yeast GGA proteins. J. Cell Biol. **151**, 587-600
17 Chidambaram, S., Zimmermann, J. and von Mollard, G. F. (2008) ENTH domain proteins are cargo adaptors for multiple SNARE proteins at the TGN endosome. J. Cell Sci. **121**, 329-338
18 Pryor, P. R., Mullock, B. M., Bright, N. A., Lindsay, M. R., Gray, S. R., Richardson, S. C. W., Stewart, A., James, D. E., Piper, R. C. and Luzio, J. P. (2004) Combinatorial SNARE complexes with VAMP7 or VAMP8 define different late endocytic fusion events. Embo R. **5**, 590-595
19 Antonin, W., Holroyd, C., Fasshauer, D., Pabst, S., Fischer von Mollard, G. and Jahn, R. (2000) A SNARE complex mediating fusion of late endosomes defines conserved properties of SNARE structure and function. EMBO J. **19**, 6453-6464
20 Hirst, J., Miller, S. E., Taylor, M. J., von Mollard, G. F. and Robinson, M. S. (2004) EpsinR is an adaptor for the SNARE protein Vti1b. Mol. Biol. Cell. **15**, 5593-5602
21 Chidambaram, S., Mullers, N., Wiederhold, K., Haucke, V. and von Mollard, G. F. (2004) Specific interaction between SNARES and epsin N-terminal homology (ENTH) domains of epsin-related proteins in trans-Golgi network to endosome transport. J. Biol. Chem. **279**, 4175-4179
22 Becherer, K. A., Rieder, S. E., Emr, S. D. and Jones, E. W. (1996) Novel syntaxin homolog, Pep12p, required for the sorting of lumenal hydrolases to the lysosome-like Vacuole in yeast. Mol. Biol. Cell. **7**, 579-594
23 Lewis, M. J. and Pelham, H. R. B. (2002) A new yeast endosomal SNARE related to mammalian syntaxin 8. Traffic. **3**, 922-929
24 Fischer von Mollard, G., Nothwehr, S. F. and Stevens, T. H. (1997) The yeast v-SNARE Vti1p mediates two vesicle transport pathways through interactions with the t-SNAREs Sed5p and Pep12p. J. Cell Biol. **137**, 1511-1524
25 Winzeler, E. and al., e. (1999) Functional characterization of the *S. cerevisiae* genome by gene deletion and parallel analysis. Science. **285**, 901-906
26 Herskowitz, I. and Jensen, R. E. (1991) Putting the HO gene to work - practical uses for mating-type switching. Methods Enzymol. **194**, 132-146
27 Berkower, C., Loayza, D. and Michaelis, S. (1994) Metabolic instability and constitutive endocytosis of *STE6*, the a-factor transporter of *Saccharomyces cerevisiae*. Mol. Biol. Cell. **5**, 1185-1198
28 Pringle, J. R. (1991) Staining of bud scars and other cell-wall chitin with calcofluor. Methods Enzymol. **194**, 732-735
29 Rothman, J. H. and Stevens, T. H. (1986) Protein sorting in yeast: mutants defective in vacuole biogenesis mislocalize vacuolar proteins into the late secretory pathway. Cell. **47**, 1041-1051
30 Babu, P., Bryan, J. D., Panek, H. R., Jordan, S. L., Forbrich, B. M., Kelley, S. C., Colvin, R. T. and Robinson, L. C. (2002) Plasma membrane localization of the Yck2p yeast casein kinase 1 isoform requires the C-terminal extension and secretory pathway function. J. Cell Sci. **115**, 4957-4968
31 Vojtek, A. and Hollenberg, S. (1995) Ras-Raf interaction: two-hybrid analysis. Methods Enzymol. **255**, 331-342
32 Dilcher, M., Veith, B., Chidambaram, S., Hartmann, E., Schmitt, H. D. and von Mollard, G. F. (2003) Use1p is a yeast SNARE protein required for retrograde traffic to the ER. Embo J. **22**, 3664-3674
33 Yeung, B. G. and Payne, G. S. (2001) Clathrin interactions with C-terminal regions of the yeast AP-1 beta and gamma subunits are important for AP-1 association with clathrin coats. Traffic. **2**, 565-576
34 Pruyne, D. and Bretscher, A. (2000) Polarization of cell growth in yeast II. The role of

the cortical actin cytoskeleton. J. Cell Sci. **113**, 571-585
35 Casamayor, A. and Snyder, M. (2002) Bud-site selection and cell polarity in budding yeast. Current Opinion in Microbiology. **5**, 179-186
36 Saint-Pol, A., Yelamos, B., Amessou, M., Mills, I. G., Dugast, M., Tenza, D., Schu, P., Antony, C., McMahon, H. T., Lamaze, C. and Johannes, L. (2004) Clathrin adaptor epsinR is required for retrograde sorting on early endosomal membranes. Dev. Cell. **6**, 525-538
37 Robinson, L. C., Bradley, C., Bryan, J. D., Jerome, A., Kweon, Y. S. and Panek, H. R. (1999) The Yck2 yeast casein kinase 1 isoform shows cell cycle-specific localization to sites of polarized growth and is required for proper septin organization. Mol. Biol. Cell. **10**, 1077-1092
38 Robinson, L. C., Menold, M. M., Garrett, S. and Culbertson, M. R. (1993) Casein kinase I-like protein-kinases encoded by YCK1 and YCK2 are required for yeast morphogenesis. Mol. Cell. Biol. **13**, 2870-2881
39 Panek, H. R., Stepp, J. D., Engle, H. M., Marks, K. M., Tan, P. K., Lemmon, S. K. and Robinson, L. C. (1997) Suppressors of YCK-encoded yeast casein kinase 1 deficiency define the four subunits of a novel clathrin AP-like complex. Embo J. **16**, 4194-4204
40 Panek, H. R., Conibear, E., Bryan, J. D., Colvin, R. T., Goshorn, C. D. and Robinson, L. C. (2000) Identification of Rgp1p, a novel Golgi recycling factor, as a protein required for efficient localization of yeast casein kinase 1 to the plasma membrane. J. Cell Sci. **113**, 4545-4555
41 Itoh, T., Koshiba, S., Kigawa, T., Kikuchi, A., Yokoyama, S. and Takenawa, T. (2001) Role of the ENTH domain in phosphatidylinositol-4,5-bisphosphate binding and endocytosis. Science. **291**, 1047-1051
42 Friant, S., Pecheur, E. I., Eugster, A., Michel, F., Lefkir, Y., Nourrisson, D. and Letourneur, F. (2003) Ent3p is a PtdIns(3,5)P-2 effector required for protein sorting to the multivesicular body. Dev. Cell. **5**, 499-511
43 Ptacek, J., Devgan, G., Michaud, G., Zhu, H., Zhu, X. W., Fasolo, J., Guo, H., Jona, G., Breitkreutz, A., Sopko, R., McCartney, R. R., Schmidt, M. C., Rachidi, N., Lee, S. J., Mah, A. S., Meng, L., Stark, M. J. R., Stern, D. F., De Virgilio, C., Tyers, M., Andrews, B., Gerstein, M., Schweitzer, B., Predki, P. F. and Snyder, M. (2005) Global analysis of protein phosphorylation in yeast. Nature. **438**, 679-684
44 Shaw, J. A., Mol, P. C., Bowers, B., Silverman, S. J., Valdivieso, M. H., Duran, A. and Cabib, E. (1991) The function of chitin synthase-2 and synthase-3 in the Saccharomyces cerevisiae cell-cycle. J. Cell Biol. **114**, 111-123
45 Ni, L. and Snyder, M. (2001) A genomic study of the bipolar bud site selection pattern in Saccharomyces cerevisiae. Mol. Biol. Cell. **12**, 2147-2170
46 Wendland, B., Steece, K. and Emr, S. (1999) Yeast epsins contain an essential N-terminal ENTH domain, bind clathrin and are required for endocytosis. EMBO J. **18**, 4383-4393
47 Brady, R. J., Wen, Y. J. and O'Halloran, T. J. (2008) The ENTH and C-terminal domains of Dictyostelium epsin cooperate to regulate the dynamic interaction with clathrin-coated pits. J. Cell Sci. **121**, 3433-3444
48 Overstreet, E., Chen, X., Wendland, B. and Fischer, J. A. (2003) Either part of a Drosophila epsin protein, divided after the ENTH domain, functions in endocytosis of delta in the developing eye. Curr. Biol. **13**, 854-860
49 Tishgarten, T., Yin, F. F., Faucher, K. M., Dluhy, R. A., Grant, T. R., von Mollard, G. F., Stevens, T. H. and Lipscomb, L. A. (1999) Structures of yeast vesicle trafficking proteins. Prot. Sci. **8**, 2465-2473
50 Dulubova, I., Yamaguchi, T., Wang, Y., Sudhof, T. C. and Rizo, J. (2001) Vam3p structure reveals conserved and divergent properties of syntaxins. Nat. Struct. Biol. **8**, 258-

264
51 Misura, K., Bock, J., Gonzalez, L. J., Scheller, R. and Weis, W. (2002) Three-dimensional structure of the amino-terminal domain of syntaxin 6, a SNAP-25 C homolog. Proc. Natl. Acad. Sci. U. S. A. **99**, 9184-9189
52 Fridmann-Sirkis, Y., Kent, H. M., Lewis, M. J., Evans, P. R. and Pelham, H. R. B. (2006) Structural analysis of the interaction between the SNARE Tlg1 and Vps51. Traffic. **7**, 182-190
53 Atlashkin, V., Kreykenbohm, V., Eskelinen, E. L., Wenzel, D., Fayyazi, A. and von Mollard, G. F. (2003) Deletion of the SNARE vti1b in mice results in the loss of a single SNARE partner, syntaxin 8. Mol. Cell. Biol. **23**, 5198-5207
54 Robinson, J. S., Klionsky, D. J., Banta, L. M. and Emr, S. D. (1988) Protein sorting in *Saccharomyces cerevisiae*: isolation of mutants defective in the delivery and processing of multiple vacuolar hydrolases. Mol. Cell. Biol. **8**, 4936-4948

Figure Legends

Fig. 1: ***ent3Δent5Δ* cells had defects in bud site selection and cell separation. A**: Diploid wild-type (WT, BY4741xBY4742) and *ent3Δent5Δ* (BKY13xSCY34) cells in logarithmic phase were fixed and stained with Calcofluor white. Cells with abnormal budding pattern were marked with arrows. **B:** Calcofluor stained diploid (WT: BY4741xBY4742, *ent3Δent5Δ*: BKY13xSCY34) and haploid (WT: BY4742, *ent3Δent5Δ*: BKY13) cells with two or more bud scars were analyzed for budding patterns. 52% of the diploid double mutant cells (SD 5.0% between two independent experiments) and 17% of WT cells (n=3, SD 4.6%) showed a non-bipolar budding pattern. For haploid cells 36% of the double mutants (n=2, SD 0.4%) and 4% of WT cells (n=3, SD 2%) with abnormal budding pattern could be observed. For each strain at least 100 cells were counted. **C**: Diploid *ent3Δent5Δ* cells had defects in cell separation resulting in a multibudded phenotype. Three layers of the same field are shown. Two non-separated cells with one additional bud each were marked with arrows. **D**: Haploid *ent3Δent5Δ* cells with defects in cell separation. Shown is an overlay of three pictures taken in different focal planes. **E:** Quantification of haploid cells with one or more buds. 2% multibudded were found in wild-type cells (BY4742 n=4, SD 1%) and 21% in *ent3Δent5Δ* cells (BKY13, n=5, SD 4%) in the haploid state. For each strain at least 150 cells were counted, non-separated cells were counted as one.

Fig. 2: ***ent3Δent5Δ* cells were defective in retrograde transport of GFP-Snc1p and missorted GFP-Yck2p**. GFP-Snc1p (**A**) and GFP-Yck2p (**B**) constructs were used to analyze the retrograde transport from early endosomes to the TGN. *ent3Δent5Δ* cells (BKY13) showed a complete mislocalization of GFP-Snc1p (pGS416) and a partly mislocalization of GFP-Yck2p (pPB2) mainly to the vacuole. **C:** GFP-Snc1p was mainly localized to the vacuolar membrane in *ent3Δent5Δ* cells (BKY13) as observed in a FM4-64 staining after 30 min incubation at 30°C. **D:** The fraction of cells with plasma membrane localized GFP-Snc1p was determined. 83% (SD 5%) of the WT cells (BY4742) showed a plasma membrane GFP-Snc1p compared to 64% (SD 9%) *ent3Δ,* 68% (SD 6%) *ent5Δ* and 4% *ent3Δent5Δ* cells (BKY13, SD 3%). Data from at least 3 experiments and at least 800 cells were used for evaluation. **E:** Quantification of cells containing a vacuolar GFP-Yck2p staining. The percentage of cells with vacuolar GFP-Yck2p was 1.9% (SD 0.2%) in BY WT (BY4742), 3.0% (SD 0.4%) in *ent3Δ*, 3.7% (SD 0.6%) in *ent5Δ* and 25.7% (SD 3.5%) in *ent3Δent5Δ*. Between 600 and 900 cells were counted from two independent experiments. Cells with any

visible vacuolar staining were counted as defective.

Fig. 3: **Three endosomal SNAREs bound to a similar interaction surface of Ent3p but used different amino acid residues. A**: Sequence alignment of Ent3p ENTH, human epsinR ENTH and Ent5p ANTH, conserved residues are boxed in gray. Position for α-helices in epsinR are indicated. Amino acid residues marked in red are exchanged in Ent3p mutant constructs. **B:** Composition of the chimera with helices α0- α5 of Ent3p, epsinR or Ent5p and α6- α8 of a different ENTH or ANTH domain. **C:** vti1b could interact with chimera D while Vti1p bound weakly to chimera C. Yeast two-hybrid VP16 activation domain constructs with chimera of Ent3p, epsinR and Ent5p domains were transformed into L40 cells together with the N-terminal domains of SNAREs fused to LexA DNA binding domain. Cells were grown on THULL plates (Vti1p) or THULL plates containing 1 mM 3-aminotriazol (Pep12p, Syn8p, vti1b). The VP16 activation domain served as negative control (pVP) for unspecific activation by LexA-SNAREs. Chimera did not cause nonspecific activation as tested in combination with a LexA-laminin fusion protein (see Supplemental Fig. 1). Expression of the constructs was confirmed by Western blotting. The positive control for vti1b was the epsinR ENTH domain. **D:** Structure modeling of Ent3p. Ent3p amino acid sequence was aligned to human epsinR crystal structure (2V8S) with 3D-Jigsaw. Helix α1 is colored blue, α8 red. Mutated amino acids were marked as ball and stick view and labeled (Pymol). **E:** Modeled Ent3p structure (red) was aligned to epsinR (blue) in complex with vti1b (orange, complex: 2qy7A). Three epsinR residues required for binding of vti1b and the corresponding residues in Ent3p (Y60, F62, R154) are indicated. The residue corresponding to Ent3p E103 is not involved in binding between epsinR and vti1b. **F:** Yeast two-hybrid assay of WT Ent3p ENTH and Ent3p ENTH mutants containing the indicated amino acid exchanges with endosomal SNAREs. Cells were streaked on THULL plates containing 2 mM 3-aminotriazol. Ent3p ENTH mutants were expressed and did not cause nonspecific activation (see Supplemental Fig. 1).

Fig. 4: **In vivo effects of Ent3p point mutants.** In a sucrose density gradient (22-55% sucrose in HEPES) the distribution of the SNAREs 3xHA-Syn8p (**A**), Vti1p (**B, C**) and Pep12p (**D**) was analyzed in homogenates from WT (BY4742), *ent5Δ*, *ent3Δent5Δ* (BKY13) and *ent3Δent5Δ* cells expressing Ent3p point mutants under the endogenous promoter (Y60D = pJZ17, E103W = pCP13, R154E = pJZ18). **C:** Quantification of the Vti1p distribution. The relative intensities of Vti1p in the gradient fractions (obtained from one representative blot per strain) was plotted against the fraction number. The distributions of the three SNAREs in *ent3Δent5Δ* cells and of Vti1p and Pep12p in *ent3Δent5Δ ent3-R154E* cells were shifted to denser fractions. Ent3p R154E did not bind any of the SNAREs. The other Ent3p mutants, which interacted with either Vti1p or Syn8p caused similar distribution to *ent5Δ* cells for all SNAREs. **E:** The GFP-Snc1p localization defect in *ent3Δent5Δ* cells (BKY13) was improved by expressing *ent3* point mutants in this strain. Data was obtained from 2 (Y60D) or 3 (F62D, E103W, R154E) experiments. At least 400 cells per strain were counted *ent5Δ* and double mutant data was copied from Fig. 2. **F:** The expression of point mutant constructs could not complement the CPY sorting defect of *ent3Δent5Δ* cells. CPY secreted onto nitrocellulose membrane was detected with mouse anti-CPY and goat anti-mouse-HRP antibodies. Low levels of secretion in *ent3-Y60D* expressing cells were due to growth defects.

Fig. 5: **Membrane binding of the Ent3p domains and their function in CPY sorting. A:** Membrane association of Ent3p domains was determined after differential centrifugation of cell homogenates (H) at 13.000 g (pellet = P13) and 200.000 g (pellet = P200, supernatant = S200). Fractionation was controlled with the soluble phosphoglycerate kinase (PGK), the ER

marker Use1p, which fractionates with P13 [32] and Vti1p which is known to fractionate with P13 and P200 [24]. Total Ent3p was determined by adding intensities in fractions P13, P200 and S200). 42% (SD 11%, n= 4) of total Ent3p was membrane associated (P13 + P200) in *ent3Δ* cells expressing *ENT3* from a *2μ* plasmid (pSC4). The Ent3p domains were expressed in *ent3Δent5Δ* cells (BKY13) from *CEN*-plasmids under control of the *TPI* promoter. In the ENTH domain expressing cells 49% (SD 12%, amino acids 1-172, pCP7) and in the HA-tagged C-terminus containing cells 20% (SD 13%, amino acids 158-408, pLS1) of the total protein were membrane bound. In cells with the Ent3p construct deficient for PI-binding 32% (SD 12%, -PI, amino acids 28-408, pCP8) of this protein was membrane associated. Western blots were incubated with antibody against the indicated proteins and against the HA-tag. **B:** CPY secretion was determined for *ent3Δent5Δ* cells (BKY13) expressing different parts of Ent3p. The Ent3p-ENTH domain (pCP7) and the C-terminus (amino acids 158-408, pCP9) alone were not able to complement the CPY secretion defect in *ent3Δent5Δ* cells. The full length Ent3p without the PI-binding ability (pCP8) could partially complement the defect compared to *ent5Δ* cells. Cells were overlaid with nitrocellulose membranes and secreted CPY detected with mouse-anti-CPY and goat-anti-mouse-HRP antibodies.

Fig. 6: **Expression of the Ent3 C-terminus suppressed GFP-Snc1p and GFP-Yck2p sorting defects in *ent3Δent5Δ* cells. A:** The Ent3p ENTH domain (BKY13 pCP7) was not able to complement the GFP-Snc1p and GFP-Yck2p sorting defects in *ent3Δent5Δ* cells. **B:** The Ent3p C-terminus (BKY13 pCP8) and Ent3p without PI binding ability (BKY13 pCP9) almost complemented the GFP-Snc1p defect to a level comparable to *ent5Δ* cells. The fraction of cells with plasma membrane localized GFP-Snc1p was determined. In *ent3Δent5Δ* cells (BKY13) expression of the ENTH domain resulted in 14% (SD 3%), of the C-terminus 50% (SD 14%) and of Ent3p without PI binding 51% (SD 3%) of cells with plasma membrane GFP-Snc1p. Data from at least 3 experiments and at least 800 cells was used for evaluation. **C:** The Ent3p C-terminus and Ent3p without PI binding ability complemented partially the GFP-Yck2p sorting defect in *ent3Δent5Δ* cells while the Ent3p ENTH domain did not improve sorting. Percentage of cells with vacuolar GFP-Yck2p (pCP29) staining: *ent3Δent5Δ* 25.7%, *ent5Δ* 3.7% (transferred from fig. 2), *ent3Δent5Δ* cells (BKY13) containing Ent3p ENTH 28.1% (SD 4.9%), -PI mutant 13.5% (SD 1.7%), C-terminus 9.8% (SD 3.8%). Between 500 and 700 cells were counted in two independent experiments.

Table 1: Yeast strains used in this study

Strain	Genotype	Reference
BY4741	*MATα his3Δ1 leu2Δ0 met15Δ0 ura3Δ0*	Euroscarf
ent5Δ	*MAT**a** his3Δ1 leu2Δ0 lys2Δ0 ura3Δ0 ent5Δ::kanMX4*	Euroscarf
ent3Δ	*MAT**a** his3Δ1 leu2Δ0 lys2Δ0 ura3Δ0 ent3Δ::kanMX4*	Euroscarf
BKY13	*MAT**a** his3Δ1 leu2Δ0 lys2Δ0 ura3Δ0 ent5Δ::kanMX4 ent3Δ::LEU2*	[21]
BY4742	*MAT**a** his3Δ1 leu2Δ0 lys2Δ0 ura3Δ0*	Euroscarf
BY4743	*MAT**a**/α his3Δ1/his3Δ1 leu2Δ0/leu2Δ0 lys2Δ0/LYS2 ura3Δ0/ura3Δ0 MET15/met15Δ0*	Euroscarf
SCY35	*MAT**a**/α his3Δ1/his3Δ1 leu2Δ0/leu2Δ0 lys2Δ0/lys2Δ0 ura3Δ0/ura3Δ0 ent5Δ::kanMX4/ent5Δ::kanMX4 ent3Δ::LEU2/ent3Δ::LEU2*	This study
SCY34	*MATα his3Δ1 leu2Δ0 lys2Δ0 ura3Δ0 ent5Δ::kanMX4 ent3Δ::LEU2*	This study
L40	*MAT**a** leu2-3,112 his3-Δ200 ade2-101 trp1-Δ901 LYS2::(lexAop)4-HIS3 URA3::(lexAop)4-lacZ gal80*	[31]
SEY6211	*MATa leu2-3,112 ura3-52 his3-Δ200 ade2-101 trp1-Δ901 suc2-Δ9 mel-*	[54]
SEY6210	*MATα leu2-3,112 ura3-52 his3-Δ200 trp1-Δ901 lys2-801 suc2-Δ9 mel*	[54]
SCY2	*MATα leu2-3,112 ura3-52 his3-Δ200 trp1-Δ901lys2-801suc2-Δ9 mel- ent3Δ::kanMX4*	[17]
SCY25	*MATα leu2-3,112 ura3-52 his3-Δ200 trp1-Δ901 lys2-801 ent5Δ::kanMX4*	[17]
SCY26	*MATa leu2-3,112 ura3-52 his3-Δ200 ade2-101 trp1-Δ901 suc2-Δ9 mel- ent3Δ::LEU2 ent5Δ::kanMX4*	[17]

Biochemical Journal Immediate Publication. Published on 26 Jul 2010 as manuscript BJ20100693

Table 2: Plasmids used in this study

Plasmid	Description	Reference
pCP7	Ent3p ENTH domain (aa 1-172) in pYX112 (*CEN, TPIp, URA3*)	This study
pCP8	Ent3p aa 28-408 in pYX112 (*CEN, TPIp, URA3*)	This study
pCP9	Ent3p C-terminus aa 158-408 in pYX112 (*CEN, TPIp, URA3*)	This study
pLS1	3xHA-Ent3p C-terminus (aa 158-408) in pYX112	This study
pSC4	*ENT3* (336 bp 5'UTR, 277 bp 3'UTR) in YEp351 (*2μ, LEU2*)	This study
pSC5	*ENT3* (336 bp 5'UTR, 277 bp 3'UTR) in pRS315 (*CEN, LEU2*)	This study
pJZ17	*ENT3* (336 bp 5'UTR, 277 bp 3'UTR) Y60D in pRS316 (*CEN, URA3*)	This study
pJZ18	*ENT3* (336 bp 5'UTR, 277 bp 3'UTR) R154E in pRS316	This study
pCP11	*ENT3* (336 bp 5'UTR, 277 bp 3'UTR) F62D in pRS316	This study
pCP13	*ENT3* (336 bp 5'UTR, 277 bp 3'UTR) E103W in pRS316	This study
pJZ21	3xHA-Syn8p (250 bp 5'UTR, 141 bp 3'UTR) in pRS313 (*CEN, HIS3*)	This study
pLexN	LexA DNA binding domain (*2μ, TRP1*)	[31]
pVP16-3	VP16 activation domain (*2μ, LEU2*)	[31]
pBK118	Vti1p N-terminus (aa 1-115) in pLexN	[21]
pBK171	Pep12p N-terminus (aa 1-200) in pLexN	[17]
pBK165	Syn8p N-terminus (aa 1-169) in pLexN	[17]
pBK111	Mouse vti1b N-Terminus (aa 1-128) in pLexN	[21]
pKW3	Ent3p ENTH domain (aa 1-172) in pVP16-3	[21]
pCW5	ChimA: Ent3p aa 1-S112 fused to Ent5p I113-172 in pVP16-3	This study
pCW6	ChimB: Ent5p aa 1-V111 fused to Ent3p aa I113-172 in pVP16-3	This study
pCW7	ChimC: Ent3p aa 1-S112 fused to epsinR aa I105-162 in pVP16-3	This study
pCW8	ChimD: epsinR aa 1-H104 fused to Ent3p aa I113-162 in pVP16-3	This study
pJZ19	Ent3p Y60D aa 1-172 in pVP16-3	This study
pJZ20	Ent3p R154E aa 1-172 in pVP16-3	This study
pAN4	Ent3p F62D aa 1-172 in pVP16-3	This study
pAN5	Ent3p E103W aa 1-172 in pVP16-3	This study
pGS416	GFP-Snc1p plasmid (*CEN, URA3*)	[15]
pCP25	GFP-Snc1p in pRS313 (*CEN, HIS3*)	This study
pPB2	GFP-Yck2p in pRS316 (*CEN, URA3*)	[30]
pCP29	GFP-Yck2p in pRS313 (*CEN, HIS3*)	This study
pSM492	3xHA epitope with BglII ends in pBluescript II	[27]
pGAL-HO	yeast endonuclease for switching the mating type (*CEN, URA3*)	[26]

Biochemical Journal Immediate Publication. Published on 26 Jul 2010 as manuscript BJ20100693

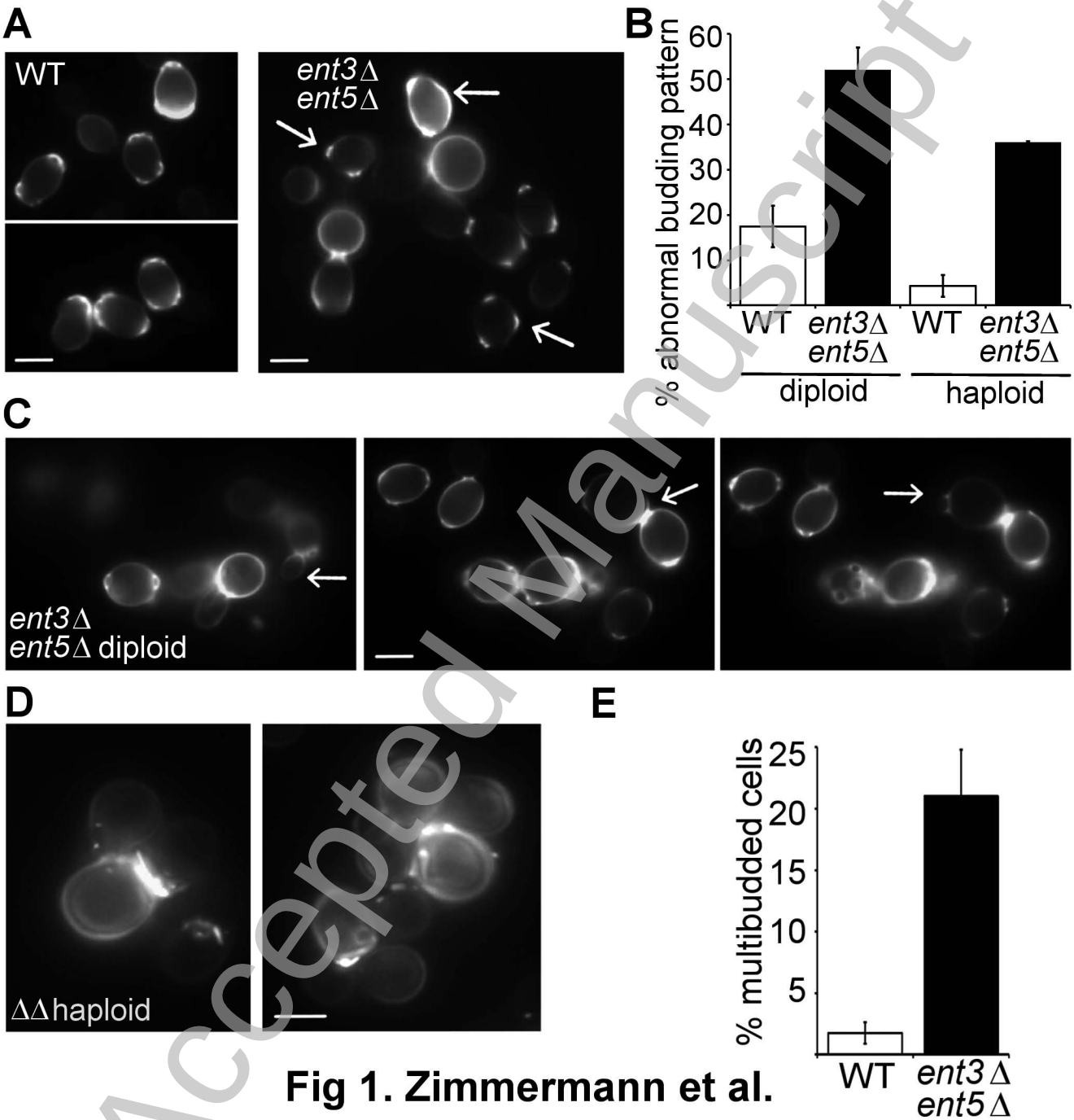

Fig 1. Zimmermann et al.

Biochemical Journal Immediate Publication. Published on 26 Jul 2010 as manuscript BJ20100693

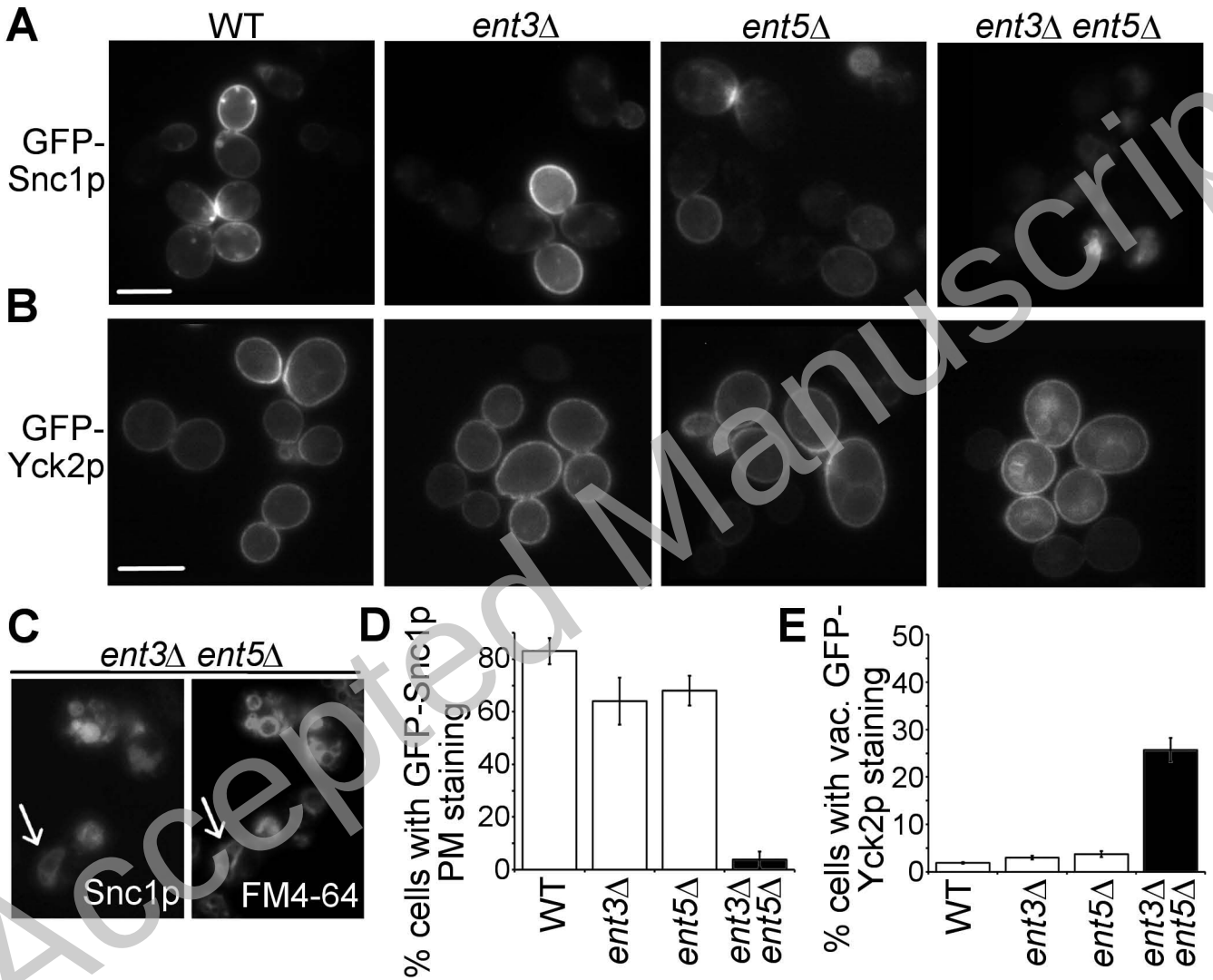

Fig. 2 Zimmermann et al.

Biochemical Journal Immediate Publication. Published on 26 Jul 2010 as manuscript BJ20100693

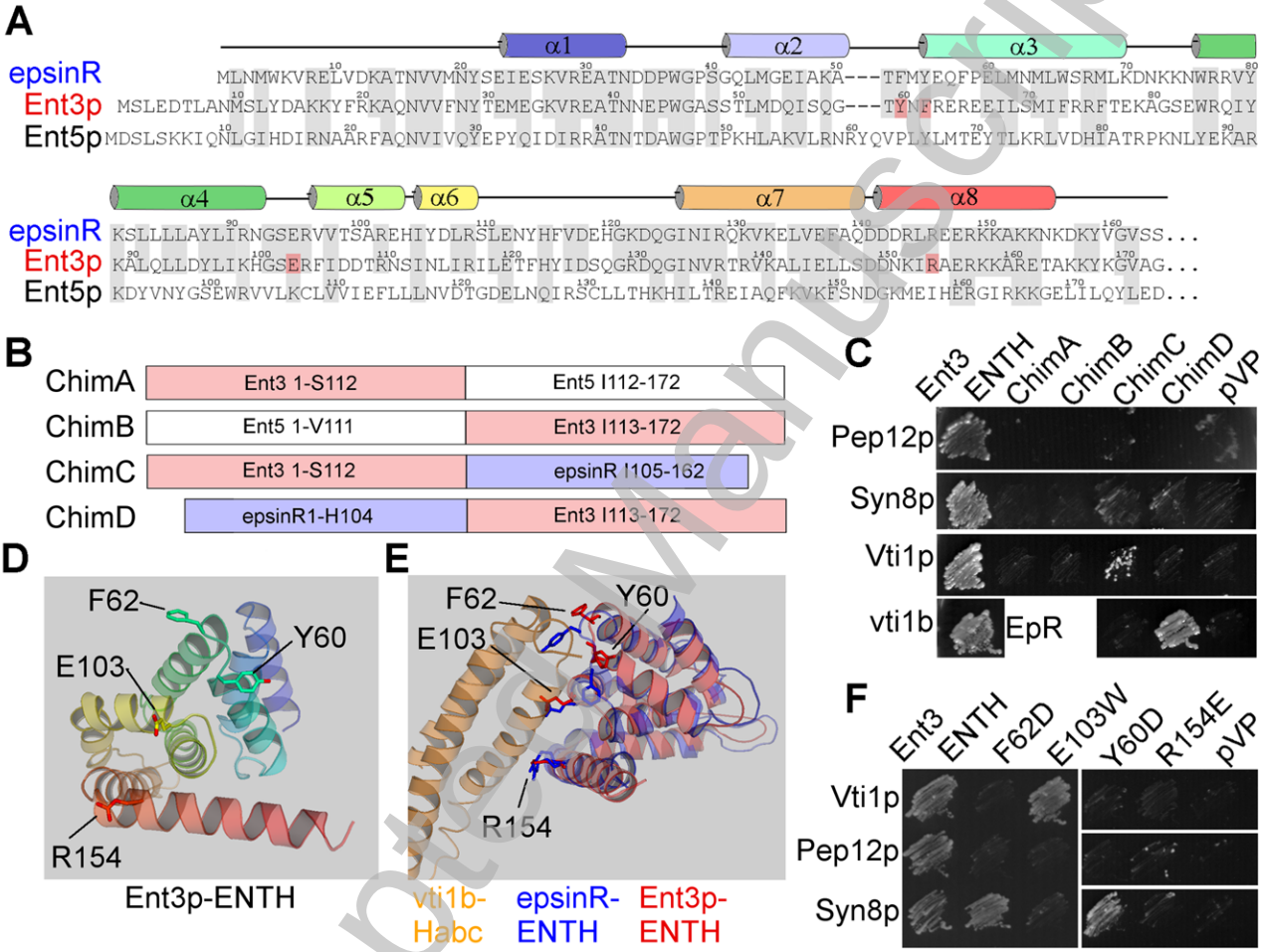

Fig. 3 Zimmermann et al.

Biochemical Journal Immediate Publication. Published on 26 Jul 2010 as manuscript BJ20100693

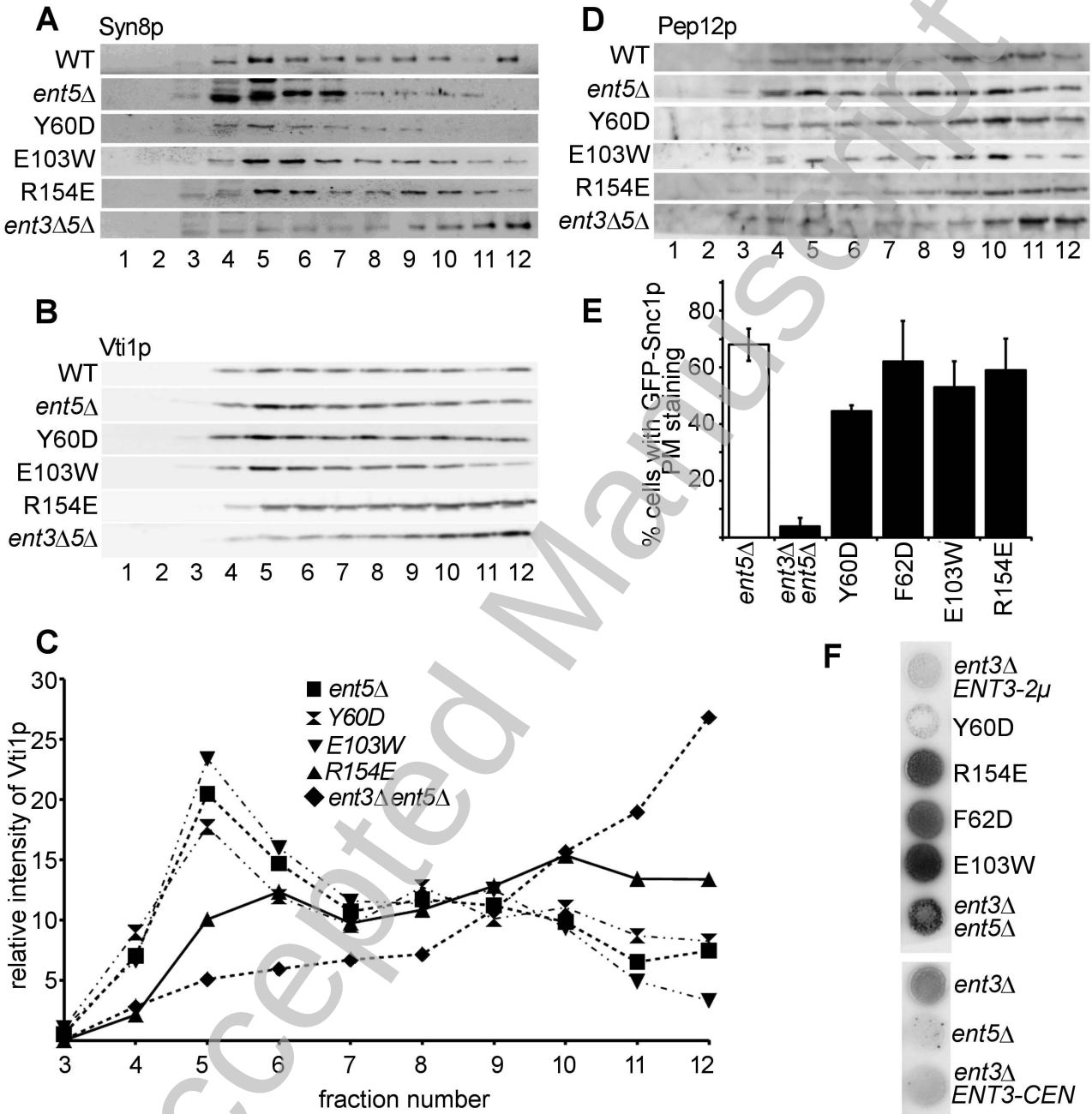

Fig. 4 Zimmermann et al.

Biochemical Journal Immediate Publication. Published on 26 Jul 2010 as manuscript BJ20100693

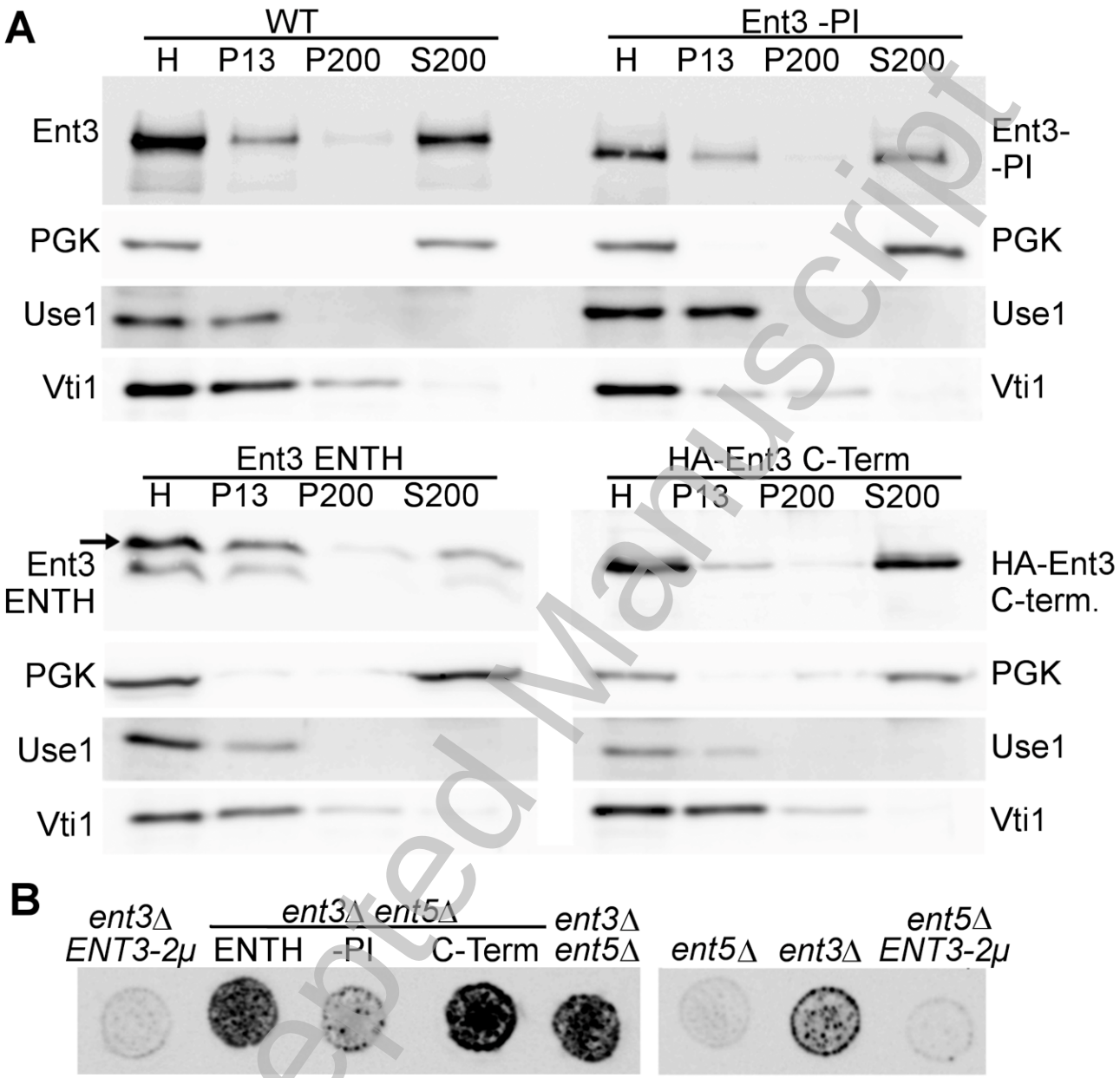

Fig. 5 Zimmermann et al.

Biochemical Journal Immediate Publication. Published on 26 Jul 2010 as manuscript BJ20100693

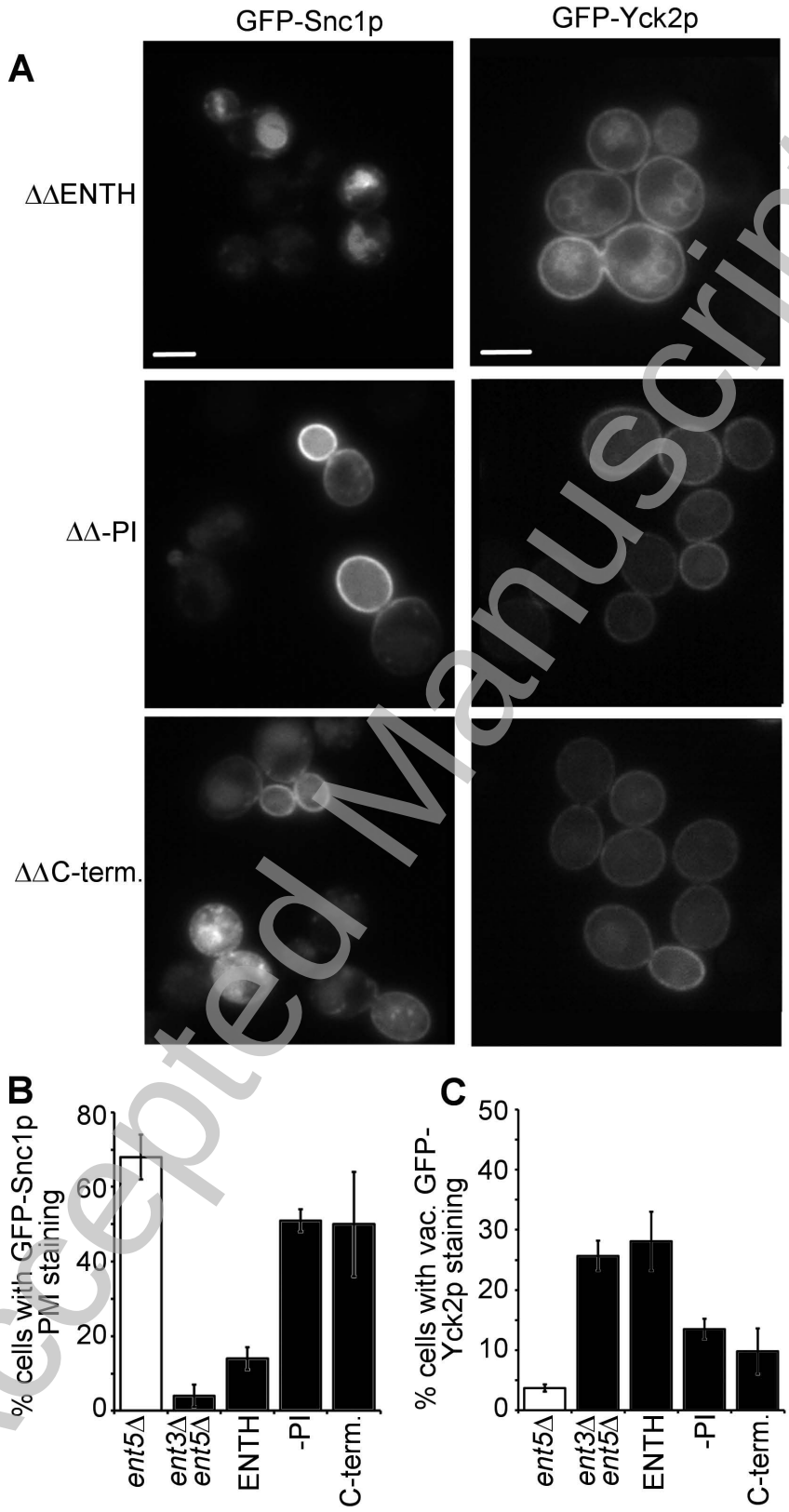

Fig. 6 Zimmermann et al.